Molecular Dynamics Simulation of Hen Egg White Lysozyme: A Test of the GROMOS96 Force Field Against Nuclear Magnetic Resonance Data

Urs Stocker and Wilfred F. van Gunsteren*
Laboratory of Physical Chemistry, ETH-Zentrum, Zürich, Switzerland

ABSTRACT **Biomolecular force fields for use in molecular dynamics (MD) simulations of proteins, DNA, or membranes are generally parametrized against ab initio quantum-chemical and experimental data for small molecules. The application of a force field in a simulation of a biomolecular system, such as a protein in solution, may then serve as a test of the quality and transferability of the force field. Here, we compare various properties obtained from two MD simulations of the protein hen egg white lysozyme (HEWL) in aqueous solution using the latest version, GROMOS96, of the GROMOS force field and an earlier version, GROMOS87+, with data derived from nuclear magnetic resonance (NMR) experiments: NOE atom–atom distance bounds, $^3J_{HN\alpha}$-coupling constants, and backbone and side-chain order parameters.**

The convergence of these quantities over a 2-ns period is considered, and converged values are compared to experimental ones. The GROMOS96 simulation shows better agreement with the NMR data and also with the X-ray crystal structure of HEWL than the GROMOS87+ simulation, which was based on an earlier version of the GROMOS force field. Proteins 2000;40:145–153. © 2000 Wiley-Liss, Inc.

INTRODUCTION

Molecular dynamics (MD) computer simulations are increasingly used to gain insight into molecular motion at the atomic level. The accuracy of the simulated properties depends primarily on the quality of the atomic interaction function or force field that is used, and on the extent of sampling of the conformational space and convergence of different quantities obtained within the simulation period. Force fields used in biomolecular simulation can be parametrized in different ways. Some force fields are parametrized using experimental data on small molecules in the condensed phase, e.g., to reproduce properties of liquids, liquid mixtures, and small molecules in solution. The parameter set obtained is then used to simulate biologically relevant molecules or molecular systems, such as proteins or DNA in solution, or membranes. To test the quality of a biomolecular force field, atomic level properties obtainable from nuclear magnetic resonance (NMR) experiments on biomolecules, such as NOE distance bounds, ^{3}J-coupling constants, or order parameters S^2, can be computed from a molecular dynamics trajectory and compared to experimental values.

With increasing theoretical and experimental knowledge and computer power biomolecular force fields also evolve and should show increased accuracy. In the present work, a 2-ns simulation of hen egg white lysozyme (HEWL) based on the GROMOS96 force field[1,2] is compared to a simulation[3] with an enhanced version, GROMOS87+[3] of the previous GROMOS87[4] force field. In an earlier study of HEWL,[3] a slight modification (GROMOS87+) of the GROMOS87 parameter set[4] was shown to improve the agreement with NMR data. Here, we show that the GROMOS96 parameter set[1,2] improves the agreement obtained in Smith et al.[3] The major differences between the latter two versions of the GROMOS force field are the following (Table I).

In the GROMOS force field, the van der Waals interaction is modeled in terms of a Lennard-Jones function, V_{LJ}, with C12 and C6 parameters,

$$V_{LJ}(r_{ij}) = \mathrm{C12}(i,j)\cdot r_{ij}^{-12} - \mathrm{C6}(i,j)\cdot r_{ij}^{-6}. \quad (1)$$

The parameters for the C12 and C6 pairwise interaction between two (united) atoms i and j at a distance $r_{ij} = |\vec{r}_i - \vec{r}_j|$ are derived from the atomic parameters by a multiplication combination rule,

$$\mathrm{C12}(i,j) = (\mathrm{C12}(i,i))^{1/2}(\mathrm{C12}(j,j))^{1/2}, \quad (2)$$

and similarly for the C6 parameters, where different values for $(\mathrm{C12}(i,i))^{1/2}$ and $(\mathrm{C12}(j,j))^{1/2}$ can be chosen when combining different atom types i and j depending on the nature (purely van der Waals or partly electrostatic) of the pairwise interaction. Calculation of the solvation free energy of alkane molecules in simple point charge (SPC) water[5] led to a change in the C12(CH_x, O_{water}) parameter because the alkane solvation energy was too favorable with the GROMOS87 force field. In addition, aromatic hydrogen atoms were treated explicitly in GROMOS87+ in order to mimic the quadrupole moment of aromatic rings. These two changes led to an improved simulation of HEWL in aqueous solution.[3] However, protein simulations using the GROMOS87 and GROMOS87+ force fields showed slightly too much motion of the amino acid peptide planes.[3,6] Therefore, in GROMOS96, the dihe-

Grant sponsor: Schweizerischer Nationalfonds; Grant number: 21-41875.94.

*Correspondence to: Wilfred F. van Gunsteren, Laboratory of Physical Chemistry, ETH-Zentrum, 8092 Zürich, Switzerland. E-mail: wfvgn@igc.phys.chem.ethz.ch

Received 31 August 1999; Accepted 18 February 2000

© 2000 WILEY-LISS, INC.

TABLE I. Major Differences Between the Three GROMOS Force Fields for Biomolecular Simulation, GROMOS87,[4] GROMOS87+,[3] and GROMOS96[1,2†]

	Force field (force field version code)		
	GROMOS87 (37C4)	GROMOS87+ (37C4+)	GROMOS96 (43A1)
Explicit treatment of aromatic H-atoms			
Charge $q_{HC} = -q_C$	—	0.14	0.10
$(C12(HC, HC))^{1/2}$	—	0.123	0.123
$(C6(HC, HC))^{1/2}$	—	0.0092	0.0092
van der Waals parameters for use in (polar, non-polar) pairs			
$(C12(OA, OA))^{1/2}$	0.8611	0.8611	1.125
$(C12(OW, OW))^{1/2}$	0.8611	1.623	1.544
van der Waals parameters for use in any pair			
$(C12(CH1, CH1))^{1/2}$	8.470	8.470	3.373
$(C6(CH1, CH1))^{1/2}$	0.1118	0.1118	0.06148
$(C12(CH2, CH2))^{1/2}$	5.944	5.944	5.077
$(C6(CH2, CH2))^{1/2}$	0.09538	0.09538	0.08429
$(C12(CH3, CH3))^{1/2}$	5.114	5.114	5.794
$(C6(CH3, CH3))^{1/2}$	0.09421	0.09421	0.09958
Dihedral angle torsional parameters for dihedrals of type -N-CH_x- and -CH_x-C-			
Force constant K_φ	0.4184	0.4184	1
Phase shift δ for -N-CH_x-	180	180	180
Phase shift δ for -CH_x-C-	0	0	0
Multiplicity m	6	6	6

†GROMOS non-bonded atom type names: HC, hydrogen bound to carbon; C, bare carbon; OA, hydroxyl, sugar or ester oxygen; OW, water oxygen; CH1, aliphatic or sugar CH-group or united atom; CH2, aliphatic or sugar CH_2-group; CH3, aliphatic or sugar CH_3-group; N, peptide nitrogen or N_ϵ in ARG; Units: charge in *e*; $(C12)^{1/2}$ in 10^{-3} $(kJmol^{-1}nm^{12})^{1/2}$; $(C6)^{1/2}$ in $(kJmol^{-1}nm^6)^{1/2}$; K_φ in $kJmol^{-1}$; δ in degree; For further explanation see text and equations 1–3. Minor differences involve the functional forms of the covalent bond-stretching and bond-angle bending interactions and the definition of charge groups between which the non-bonded interaction is calculated.

TABLE II. Major Differences between the Simulation Parameters and Set-up of the Previous[3] and Present MD Simulations of HEWL†

	Simulation of HEWL: force field (version code)	
	Previous[3]: GROMOS87+ (37C4+)	Present: GROMOS96 (43A1)
Number of atoms or molecules		
Solute atoms	1,321	1,322
Water molecules	4,463	7,113
Counter ions (Cl^-)	0	9
Total	14,710	22,670
Truncated octahedron box length (nm)	6.71	7.7392
PDB code starting structure	2LZT	1AKI
Simulation length (ps)	1,100	2,000
Simulation time step (fs)	2	2
Treatment of long range forces		
Pair-list cut-off radius R_{cp} (nm)	0.8	0.8
Pair-list update frequency (ps^{-1})	100	100
Non-bonded interaction cut-off R_{cl} (nm)	1.4	1.4
Poisson-Boltzmann reaction field (PBRF)	No	Yes
Beyond radius R_{rf}(nm)	—	1.4
Using relative dielectric permittivity ϵ_{rf}	—	54

†See also Table I and text. PDB, protein data bank.

dral angle force constant K_φ for the φ, ψ backbone dihedrals was redetermined and slightly (about $k_BT/4$) increased. The dihedral angle force is the negative derivative with respect to coordinates of the dihedral angle potential energy term

$$V^{trig}(\varphi) = K_\varphi[1 + \cos(\delta)\cos(m\varphi)] \quad (3)$$

in which δ is a phase shift (0 or 180°) and m is the multiplicity (6 for φ and ψ) of the selected dihedral angle φ. Finally, the van der Waals parameters of CH_x united atoms were redetermined by fitting of the simulated heat of vaporization and density to experimental values for liquid *n*-alkanes.[7] The major differences between the

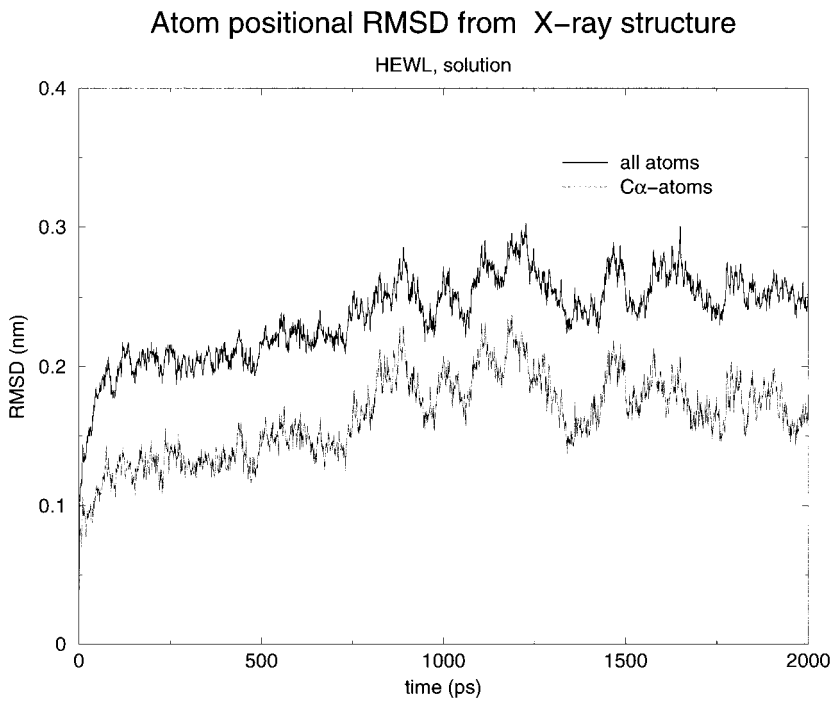

Fig. 1. Root-mean-square atom positional deviation (RMSD) in nm from the X-ray (crystal) structure[9] as function of time in ps for the simulation of HEWL using the GROMOS96 force field. Rotational and translational fitting was applied using all 129 Cα atoms. RMSD of Cα atoms (dotted line) and of all atoms (solid line) are shown.

TABLE III. NOE Distances and Bound Violations Computed from MD Trajectories and Experimentally Determined NOE Distance Bounds (1158)†

	Number of violations			Mean violation:
	>0.05 nm	>0.1 nm	>0.3 nm	$R_E - R_0$
GROMOS87+ simulation (W2[3]) (300–1,100 ps)	94	54	7	0.14
GROMOS96 simulation (300–1,100 ps)	77	45	8	0.11
GROMOS96 simulation (1,200–2,000 ps)	88	65	14	0.14
GROMOS96 simulation (300–2,000 ps)	75	49	10	0.12

	Examples of NOE violations								
	Exp. NMR data	GROMOS87+ 300–1,100 ps		GROMOS96 300–1,100 ps		GROMOS96 1,200–2,000 ps		GROMOS96 300–2,000 ps	
NOE pair	exp R_0	R_E	$R_E - R_0$	R_E	$R_E - R_0$	R_E	$R_E - R_0$	R_E	$R_E - R_0$
2Hγ2 − 38HN	0.40	0.58	0.18	0.79	0.39	0.76	0.36	0.78	0.38
8Hγ − 17Hγ	0.47	1.04	0.57	0.97	0.50	0.99	0.52	0.98	0.51
15Hε1 − 88Hγ1	0.54	0.95	0.41	0.73	0.19	0.85	0.31	0.78	0.24
15Hε1 − 88Hδ	0.40	0.84	0.44	0.62	0.22	0.82	0.42	0.70	0.30
23Hζ − 104HN	0.76	1.13	0.37	0.58	0	0.53	0	0.56	0
28Hε3 − 88Hδ	0.85	0.91	0.06	1.19	0.34	0.64	0	0.65	0
92Hγ2 − 96Hα	0.40	0.64	0.24	0.87	0.47	0.87	0.47	0.87	0.47
95Hα − 108Hζ2	0.30	0.68	0.38	0.62	0.32	0.61	0.31	0.62	0.32
95Hβ − 108Hζ2	0.40	0.85	0.45	0.75	0.35	0.75	0.35	0.75	0.35
95Hβ − 108Hη2	0.35	0.84	0.49	0.73	0.38	0.78	0.43	0.75	0.40
99Hβ − 108Hζ3	0.45	0.74	0.29	0.85	0.40	0.86	0.41	0.84	0.39

†Results are given for an earlier simulation[3] and three analysis periods of the present simulation. R_0 is the experimentally determined distance bound.[19–21] R_E is the distance from the trajectory using r^{-3} averaging. The symbol R_E-R_0 indicates a (mean) violation, calculated as a mean of the larger value of R_E-R_0 and zero. Therefore, 0 indicates no violation. Distances and NOE bounds are in nm.

GROMOS87,[4] GROMOS87+,[3] and GROMOS96[1,2] force fields have been summarized in Table I.

A second condition for obtaining accurate prediction of properties from a molecular simulation is sufficient sampling of conformational space, leading to converged values of different atomic and molecular or system properties.[8] Here, the convergence of calculated NOE distance bounds, ^{3}J-coupling constants, and main- and side-chain ^{1}H-^{15}N order parameters are analyzed by calculating the selected property using different parts of the simulation trajectory

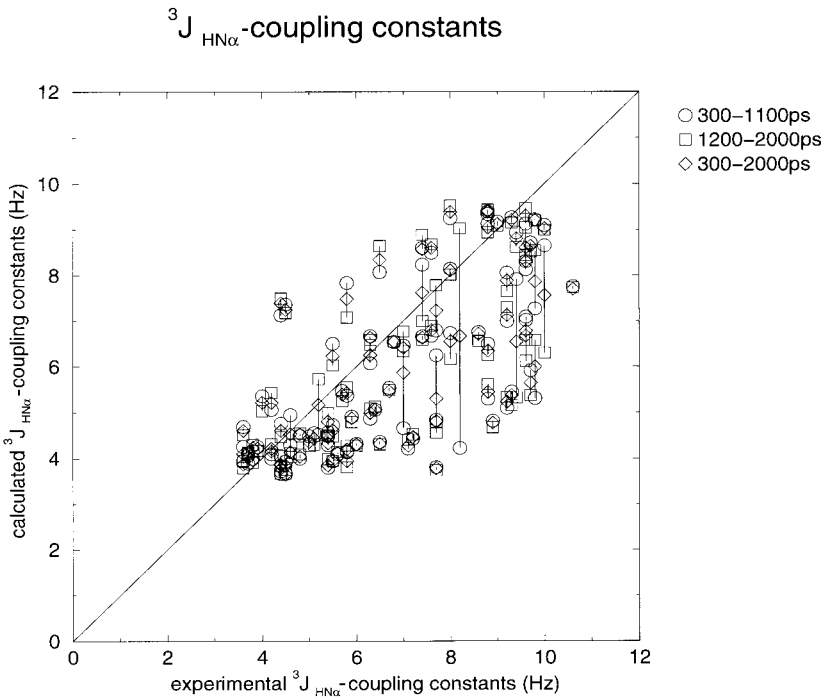

Fig. 2. Comparison of 95 experimental[19] and calculated $^3J_{HN\alpha}$-coupling constants (in Hz) averaged over different time windows: ○ 300–1,100 ps; □ 1,200–2,000 ps; ◇ 300–2,000 ps. Corresponding calculated $^3J_{HN\alpha}$-coupling constants are connected with lines.

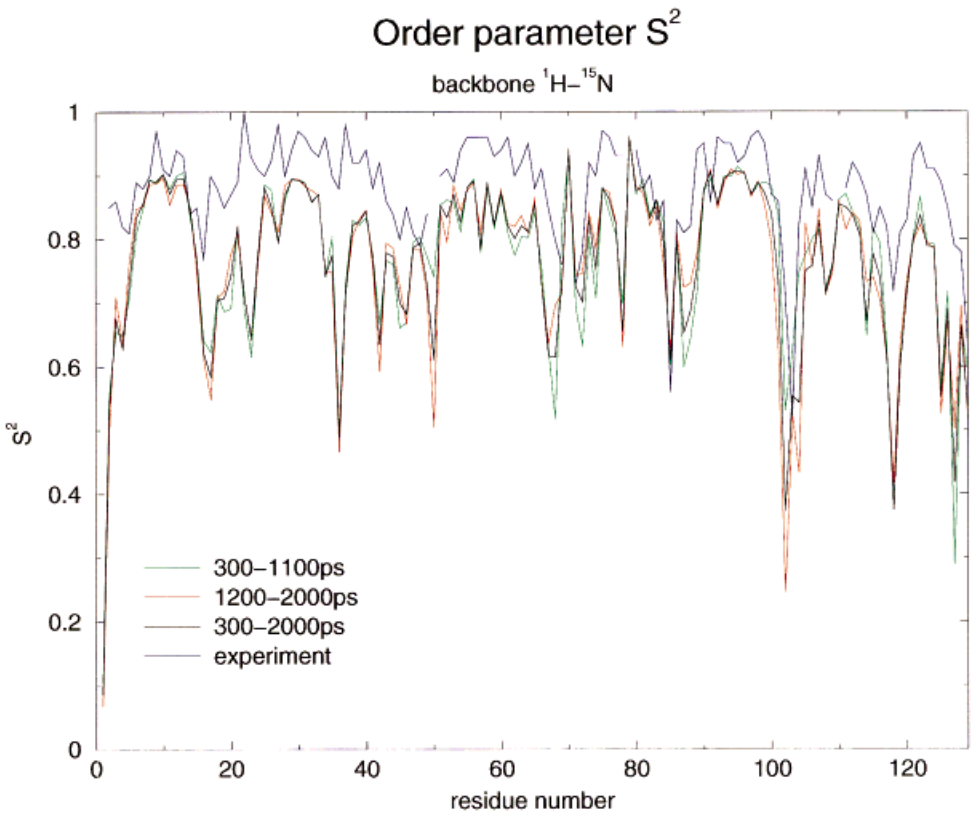

Fig. 3. Backbone ^1H-^{15}N order parameters (S^2) as function of residue number. Averages calculated using a 200-ps averaging window moving through different analysis time periods are shown together with experimental data.[21] There is no experimental value available for residues LYS1, SER50, PRO70, PRO79, and ALA110. Blue line, exp; green line, 300–1,100 ps; red line, 1,200–2,000 ps; black line, 300–2,000 ps.

and time averages extending over 800 ps and 1,700 ps. When comparing the properties of HEWL calculated with the GROMOS96 force field to the ones calculated in Smith et al.,[3] using the GROMOS87+ force field, the trajectory between 300 ps and 1,100 ps was used as in Smith et al.[3]

METHODS

Lysozyme consists of 129 amino acids with 1,001 non-hydrogen atoms. Hydrogen atoms attached to aliphatic carbon atoms are incorporated into these (the united atom

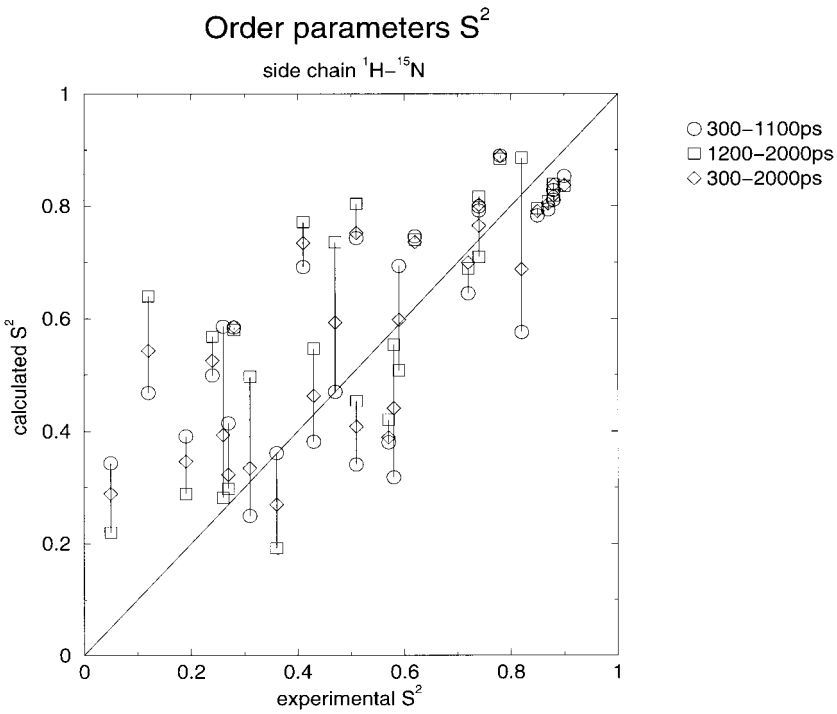

Fig. 4. Comparison of 28 experimental[21] ^{1}H-^{15}N order parameters (S^2) of side chain NH groups with values calculated using a 200-ps averaging window moving through different time periods: ○ 300–1,100 ps; □ 1,200–2,000 ps; ◇ 300–2,000 ps. Corresponding calculated S^2 are connected with lines. For NH_2 groups the average of the order parameters for the two NH vectors is displayed.

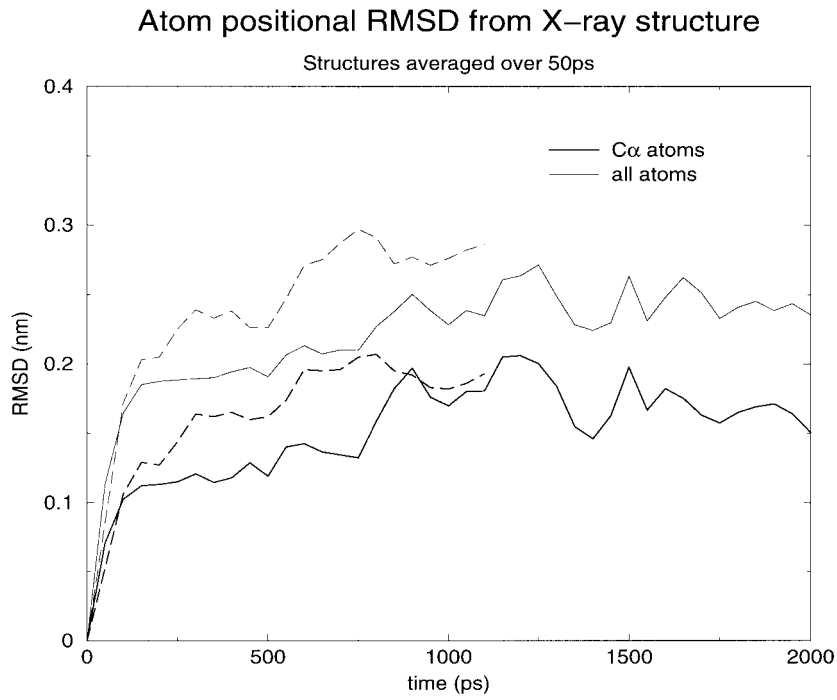

Fig. 5. Root-mean-square atom positional deviation (RMSD) in nm from the X-ray (crystal) structure as function of time in ps. Rotational and translational fitting was applied using all 129 Cα atoms. Structures were averaged over 50-ps windows. RMSD of Cα atoms (thick line) and of all atoms (thin line) of these averages are shown for the present (GROMOS96) simulation (solid lines, 2,000 ps) and the earlier (GROMOS87+ (W2)) simulation[3] (dashed lines, 1,100 ps).

approach), and the remaining 321 hydrogen atoms are treated explicitly. The protein was simulated at pH 6. The amino acids GLU and ASP were taken to be deprotonated, and LYS, ARG, and HIS residues were protonated, leading to a charge of +9 electron charges per chain. The crystal structure of lysozyme (entry 1AKI[9] of the Brookhaven Protein Database[10]) determined at 1.5 Å resolution[11] was used as a starting structure. Truncated octahedron boundary conditions were used with a box length of 7.7392 nm between the quadratic surfaces. Seven thousand one hundred twenty-two SPC water molecules[5] were added from an equilibrated cubic box containing 216 water molecules.[1] The added water molecules were selected such that no water oxygen atom is closer than 0.23 nm to a non-hydrogen atom of the protein or another water oxygen atom. The system, protein and water, was initially energy minimized for 100 cycles using the steepest descent method. The protein atoms were harmonically restrained[1] to their

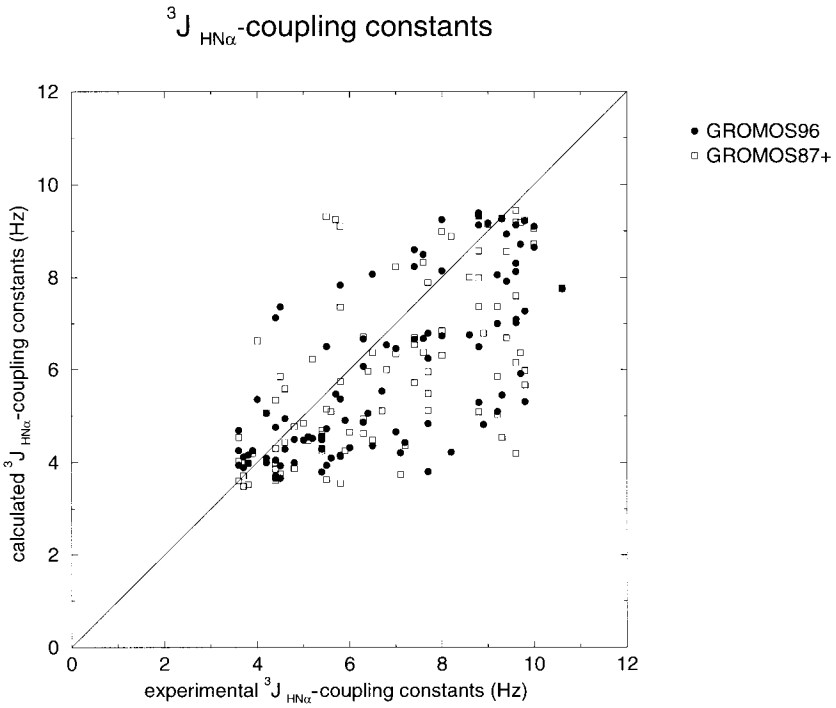

Fig. 6. Comparison of 95 experimental[19] and calculated $^3J_{HN\alpha}$-coupling constants for the GROMOS96 (●) and the GROMOS87+ (□) simulations, averaged over 300–1,100 ps.

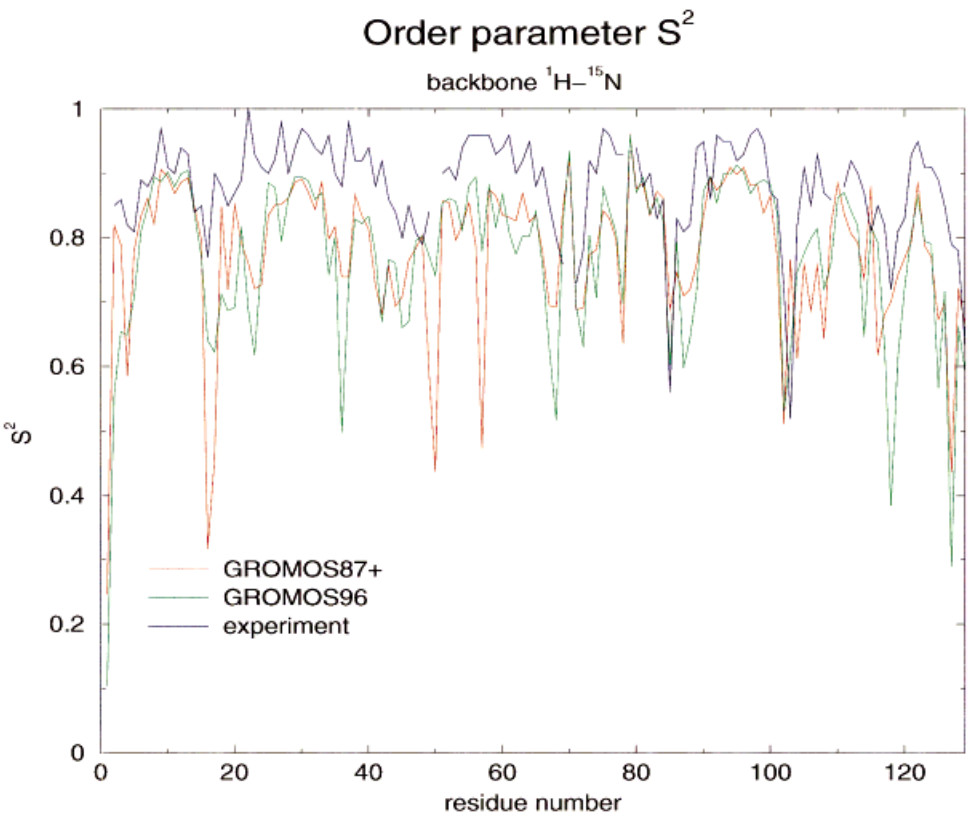

Fig. 7. Backbone ^1H-^{15}N order parameters (S^2) as a function of residue number. The values determined over the 300–1,100 ps periods of the GROMOS87+ and GROMOS96 simulations are compared with experimental data.[21] There is no experimental value available for residues LYS1, SER50, PRO70, PRO79, and ALA110. Blue line, exp; green line, GROMOS96; red line, GROMOS87+.

initial positions with a force constant of 25,000 kJ/(mol nm^2). The minimized structure was then pre-equilibrated in a short MD run of 100 steps of 0.002 ps, still restraining protein atom positions. Initial velocities were assigned from a Maxwell-Boltzmann distribution at 300K. Protein and solvent were coupled separately to temperature baths

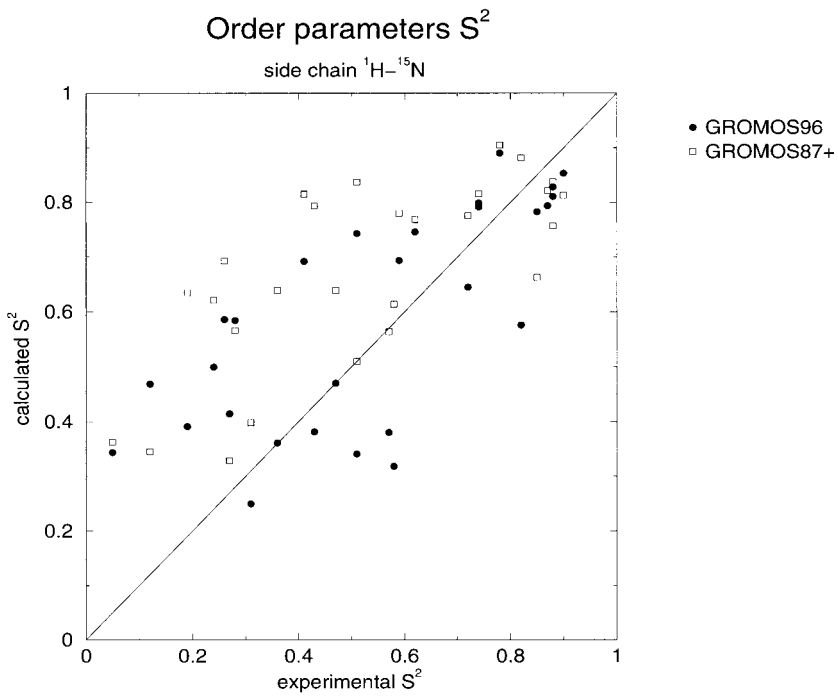

Fig. 8. Comparison of 28 experimental[21] ^{1}H-^{15}N order parameters S^2 of side-chain NH groups with values calculated using the 300–1,100 ps period of the GROMOS96 (●) and GROMOS87+ (□) simulations. For NH_2 groups the average of the order parameters for the two NH vectors is displayed.

of 300K with a coupling time of 0.1 ps.[12] No pressure coupling was applied. A follow-up simulation (results not shown) including pressure coupling showed no significant change in the box volume. Bonds were kept rigid using the SHAKE method[13] with a relative geometric tolerance of 10^{-4}. Long-range forces were treated using twin-range cutoff radii $R_{cp} = 0.8$ nm for the charge group[1] pair list and $R_{cl} = 1.4$ nm for the longer-range non-bonded[14] interactions. The pair list for the (short-range) non-bonded interactions and the longer-range forces were updated every 10 fs. Reaction-field forces were included,[15] originating from a dielectric continuum beyond a radius of $R_{rf} = 1.4$ nm using a self-consistent relative dielectric permittivity $\epsilon_{rf} = 54$ for SPC water.[16] Nine counter ions were added by replacing water molecules. The water molecule having the highest electrostatic field at the water oxygen site, after the successive placement of previous ions, was replaced by a chloride anion. After having introduced the ions, the energy was again minimized using 100 steps of steepest descent and protein atom position constraining. The total size of the system was 1,322 protein atoms, nine chloride anions, and 7,113 water molecules, leading to a total system size of 22,670 atoms. The simulation was carried out over 2 ns with a time step of 0.002 ps. Every 500th step, the configuration was saved. The first 300 ps of the simulation was treated as the equilibration period, and different time periods of the remaining 1.7 ns were used for analysis. All simulations were performed using the GROMOS96 package and force field.[1,17]

The 1,158 NOE distances, the 95 $^{3}J_{HN\alpha}$-coupling constants, and the 124 backbone and 28 side-chain S^2 order parameters were calculated from the trajectory as in Smith et al.[3] However, it has been argued recently[18] that the S^2 order parameters should be calculated using a 200-ps averaging window (moving through the analysis period of the trajectory), which approximates the time scale of the N–H bond vector motions which determine the S^2 order parameters as derived from the NMR experiments for HEWL. Therefore, order parameters were calculated using a 200-ps averaging window, which is moved through a given analysis time period. The experimental values were taken from Smith et al.;[19,20] Buck et al.[21]

We note that the GROMOS96 simulation differs from the GROMOS87+ simulation not only in the force field version that is used (Table I), but also in a few other aspects (see Table II): more solvent molecules, the presence of counter ions, and the use of a reaction-field force induced by a dielectric continuum with $\epsilon_{rf} = 54$ beyond a 1.4-nm cut-off radius. So, strictly speaking, the combined effects of these differences between the two simulations considered here are analyzed.

RESULTS

Convergence of Calculated Properties

In Figure 1, the root-mean-square deviation (RMSD) of the GROMOS96 simulated structure from the X-ray structure is shown. After an initial increase, a first plateau is reached, where the RMSD stabilizes at 0.14 nm for Cα atoms and 0.21 nm for all atoms. The plateau reaches from 100 ps to 700 ps. After that, the RMSD increases to 0.18 nm for Cα atoms and 0.26 nm for all atoms. After 800 ps, until the end of the simulation at 2,000 ps, the values fluctuate around these values.

NOE distance bound violations are summarized in Table III. The average over the final 800 ps of the simulation shows more and larger violations than the one over 300–1,100 ps. Also the mean violation increases. As for calculating distance violations, r^{-3} averaging is used. A

few configurations with a low r-distance strongly determine the average, and violations do not increase significantly comparing the periods 300–1,100 ps and 300–2,000 ps. The r^{-3} averaging makes NOE distance violations a quickly converging property of the system.

Most of the 95 $^3J_{HN\alpha}$-coupling constants do not change very much between the two 800-ps analysis periods (Fig. 2). Exceptions are the coupling constants of residues VAL2 (10.0 Hz), ASN65 (9.4 Hz), ASP101 (7.0 Hz), and ASN103 (8.2 Hz). Also the coupling constants from the final 1,700 ps, the whole analysis period, are, except for the mentioned residues, close to the ones from the shorter periods. Torsional angle librations within a potential energy well have a small effect on mean calculated ^{3}J-coupling constants.[22] So, if no jumps over rotational barriers occur, averaged ^{3}J-coupling constant values are converged on a subnanosecond to nanosecond time scale.

The same holds for backbone ^{1}H-^{15}N order parameters (S^2). S^2 values calculated for different time periods (Fig. 3) are very similar to each other with a handful of exceptions. This behavior is expected for N–H bond vectors that sample the same region of configuration space in both of the shorter analysis periods. If the order parameter of the longer analysis period is about the average of the ones for the two 800-ps subperiods, the extent of motion in one of the two subperiods (the one with low S^2 values) encompasses the extent of motion in the other subperiod. For some residues, e.g., ARG68, SER72, ASP87, or CYS127, the first subperiod shows larger disorder; for other residues, e.g., SER50, GLY102, or GLY104, the second subperiod does.

Order parameters of ^{1}H-^{15}N bonds in side chains (Fig. 4) calculated using different analysis time periods differ more from one another than in the backbone. This reflects the larger mobility, and thus, that a larger region of configuration space is accessible to these bond vectors. Some of the values (e.g., TRP28(0.90), ASN46(0.62), ASN59(0.78), or TRP61(0.28), experimental S^2 values between parentheses) are converged within 800 ps, indicating sufficient sampling for the particular side chain, but for other residues (e.g., GLN57(0.82), ASN103(0.26), or ASN113(0.47)), sampling periods longer than a few nanoseconds are required.

Comparison of the GROMOS87+ and GROMOS96 Simulations With Experimental Data

When comparing the 2,000-ps GROMOS96 simulation with the 1,100-ps GROMOS87+ simulation of Smith et al.,[3] a corresponding analysis period, 300–1,100 ps, is used, if not stated otherwise. The atom positional RMSD from the X-ray structure (Fig. 5) is smaller in the GROMOS96 simulation than in the GROMOS87+ one, showing that the reengineered force field keeps the trajectory closer to the experimentally derived crystal structure. If structures are averaged over 50-ps windows and the atom positional RMSD from the X-ray structure is calculated for these averaged structures (Fig. 5), high-frequency motions are averaged out and the RMSD values decrease slightly compared to when single structures are considered (Fig. 1). In this case, the average RMSD values for the 800–2,000 ps period are 0.18 nm for Cα atoms and 0.24 nm for all atoms.

For NOE distance violations, an improvement compared to the previous simulation is observed (Table III). For the GROMOS96 simulation, the average violation is 0.011 nm compared to 0.014 nm for the GROMOS87+ simulation.

$^3J_{HN\alpha}$-coupling constants calculated in the GROMOS96 simulation reproduce the 95 experimental values with a RMSD of 1.72 Hz compared to 1.83 Hz in the GROMOS87+ simulation (Fig. 6). These values depend on the potential energy force field term for the backbone dihedral angle φ, for which the force constant was slightly increased between the two force fields used. The correlation coefficient between simulated and experimental J-values is 0.64 for GROMOS87+ and 0.71 for GROMOS96.

Backbone order parameters (Fig. 7) also show some improvement from the GROMOS87+ simulation to the GROMOS96 simulation when compared with experimentally derived S^2 values. The values in regions of stable secondary structure elements are well reproduced in both simulations, except for the β-sheet region (residues 42ALA-60SER), where GROMOS96 yields better results.

The side-chain order parameters calculated from the GROMOS87+ and GROMOS96 simulations (Fig. 8) show a similar degree of agreement with experimental data. The RMSD from experimental values for the 28 side-chain order parameters is 0.23 for GROMOS87+ and 0.18 for GROMOS96, respectively. Side-chain order parameters calculated from the GROMOS87+ simulation are generally a bit higher than experimentally derived order parameters. Side-chain order parameters are more sensitive to the length of the averaging period (Fig. 4). So, better agreement with experiment is to be expected not only from force field improvement, but also from longer averaging periods.

DISCUSSION

Although continually increasing computer power enables increasingly longer simulations of biomolecular systems, such as proteins or DNA in solution, and membranes, the attainable simulation periods are still too short, a few nanoseconds, for all system and atomic properties to converge. Fast relaxing properties, such as system energies and the macromolecular radius of gyration (results not shown) generally converge within a few 100 ps. The atom-positional RMSD from the starting (X-ray) structure usually converges after a nanosecond. Properties depending on rare structural transitions may even take longer to converge and are, therefore, still out of simulation range. $^3J_{HN\alpha}$-coupling constants and backbone ^{1}H-^{15}N order parameters generally converge within 1–2 ns, whereas the sampling for order parameters of side-chain bonds needs longer time.[8]

The GROMOS96 force field is able to maintain the experimentally derived X-ray structure better than the previous versions (GROMOS87, GROMOS87+) of the force field. This is due to the improvement made in the

GROMOS force field: (i) The packing of aromatic rings has been improved by the introduction of explicit hydrogens with partial charges generating a quadrupole moment; (ii) The balance between apolar–apolar, apolar–polar, and polar–polar pair interactions has been improved by a refitting of van der Waals parameters to liquid data[7]; (iii) The mobility of φ and ψ torsional angles has been slightly reduced by a slight increase of the torsional angle interaction force constants.

The agreement with the 1158 NOE bounds derived from experiment is only marginally improved going from the GROMOS87+ to the GROMOS96 force field. This is not surprising because satisfying NOE bounds is not very sensitive to details of a force field. As expected, the 95 experimental $^3J_{HN\alpha}$-coupling constants, the 124 order parameters for the backbone, and the 28 side-chain order parameters are slightly better reproduced by the GROMOS96 force field than by the GROMOS87+ one.

The present results for hen egg white lysozyme illustrate the progress that is still being made in the field of force field development for biomolecular systems. They also illustrate the different sensitivities of different quantities to particular changes in force field parameters and to the extent of sampling of conformational space.

ACKNOWLEDGMENTS

The authors wish to thank Katrin Spiegel and Dr. Lorna J. Smith for making data available and for useful discussions.

REFERENCES

1. van Gunsteren WF, Billeter SR, Eising AA, Hünenberger PH, Krüger P, Mark AE, Scott WRP, Tironi IG. Biomolecular simulation: The GROMOS96 manual and user guide. Zürich, Switzerland: Vdf Hochschulverlag; 1996.
2. van Gunsteren WF, Daura X, Mark AE. GROMOS force field. Encyclopaedia of Comput Chem 1998;2:1211–1216.
3. Smith LJ, Mark AE, Dobson CM, van Gunsteren WF. Comparison of MD simulations and NMR experiments for hen lysozyme: analysis of local fluctuations, cooperative motions and global changes. Biochemistry 1995;34:10918–10931.
4. van Gunsteren WF, Berendsen HJC. Groningen molecular simulation (GROMOS) library manual. Groningen, The Netherlands; Biomos; 1987.
5. Berendsen HJC, Postma JPM, van Gunsteren WF, Hermans J. Interaction models for water in relation to protein hydration. In: Pullman B, editor. Intermolecular forces. Dordrecht: Reidel; 1981. p 331–342.
6. Smith PE, van Schaik RC, Szyperski T, Wüthrich K, van Gunsteren WF. Internal mobility of the basic pancreatic trypsin inhibitor in solution: a comparison of NMR spin relaxation measurements and molecular dynamics simulation. J Mol Biol 1995; 246:356–365.
7. Daura X, Mark AE, van Gunsteren WF. Parametrization of aliphatic CH_n united atoms of GROMOS96 force field. J Comput Chem 1998;19:535–547.
8. van Gunsteren WF, Hünenberger PH, Mark AE, Smith PE, Tironi IG. Computer simulations of protein motion. Comp Phys Commun 1995;91:305–319.
9. Carter D, He J, Ruble JR, Wright B. The structure of the orthorhombic form of hen egg-white lysozyme at 1.5 Ångstrøms resolution. Protein Data Bank, entry 1AKI; 1997.
10. Bernstein FC, Koetzle TF, Williams GJB, Meyer EF Jr, Brice MD, Rodgers JR, Kennard O, Shimanouchi T, Tasumi M. The protein data bank: a computer-based archival file for macromolecular structures. J Mol Biol 1977;112:535–542.
11. Artymiuk PJ, Blake CCF, Rice DW, Wilson KS. The structures of the monoclinic and orthorhombic forms of hen egg-white lysozyme at 6 Å resolution. Acta Cryst Sect B 1982;38:778–783.
12. Berendsen HJC, Postma JPM, van Gunsteren WF, DiNola A, Haak JR. Molecular dynamics with coupling to an external bath. J Chem Phys 1984;81:3684–3690.
13. Ryckaert J-P, Ciccotti G, Berendsen HJC. Numerical integration of the cartesian equations of motion of a system with constraints: molecular dynamics of n-alkanes. J Comput Phys 1977;23:327–341.
14. van Gunsteren WF, Berendsen HJC. Computer simulations of molecular dynamics: methodology, applications and perspectives in chemistry. Angew Chem Int Ed Engl 1990;29:992–1023.
15. Tironi IG, Sperb R, Smith PE, van Gunsteren WF. A generalized reaction field method for molecular dynamics simulations. J Chem Phys 1995;102:5451–5459.
16. Smith PE, van Gunsteren WF. Consistent dielectric properties of the simple point charge and extended simple point charge water models at 277 and 300K. J Chem Phys 1994;100:3169–3174.
17. Scott WRP, Hünenberger PH, Tironi IG, Mark AE, Billeter SR, Fennen J, Torda AE, Huber T, Krüger P, van Gunsteren WF. The GROMOS biomolecular simulation program package. J Phys Chem A 1999;103:3596–3607.
18. Evenäs J, Forsén S, Malmendahl A, Akke M. Backbone dynamics and energetics of a calmodulin domain mutant exchanging between closed and open conformations. J Mol Biol 1999;289:603–617.
19. Smith LJ, Sutcliffe MJ, Redfield C, Dobson CM. Analysis of ϕ and χ_1 torsion angles for hen lysozyme in solution from ^{1}H NMR spin-spin coupling constants. Biochemistry 1991;30:986–996.
20. Smith LJ, Sutcliffe MJ, Redfield C, Dobson CM. Structure of hen lysozyme in solution. J Mol Biol 1993;229:930–944.
21. Buck M, Boyd J, Redfield C, MacKenzie DA, Jeenes DJ, Archer DB, Dobson CM. Structural determinants of protein dynamics: analysis of ^{15}N NMR relaxation measurements for main-chain and side-chain nuclei of hen egg white lysozyme. Biochemistry 1995;34:4041–4055.
22. Hoch JC, Dobson CM, Karplus M. Vicinal coupling constants and protein dynamics. Biochemistry 1985;24:3831–3841.